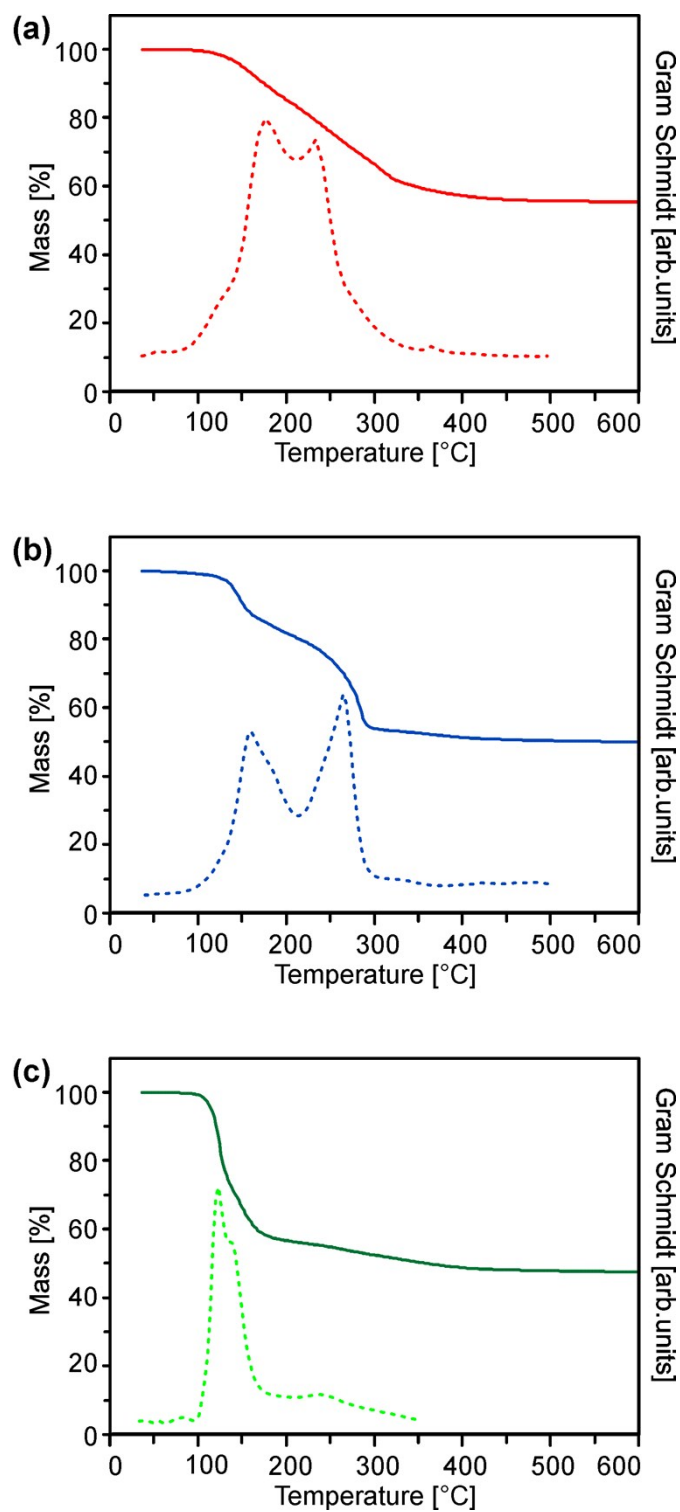


SUPPLEMENTARY MATERIAL

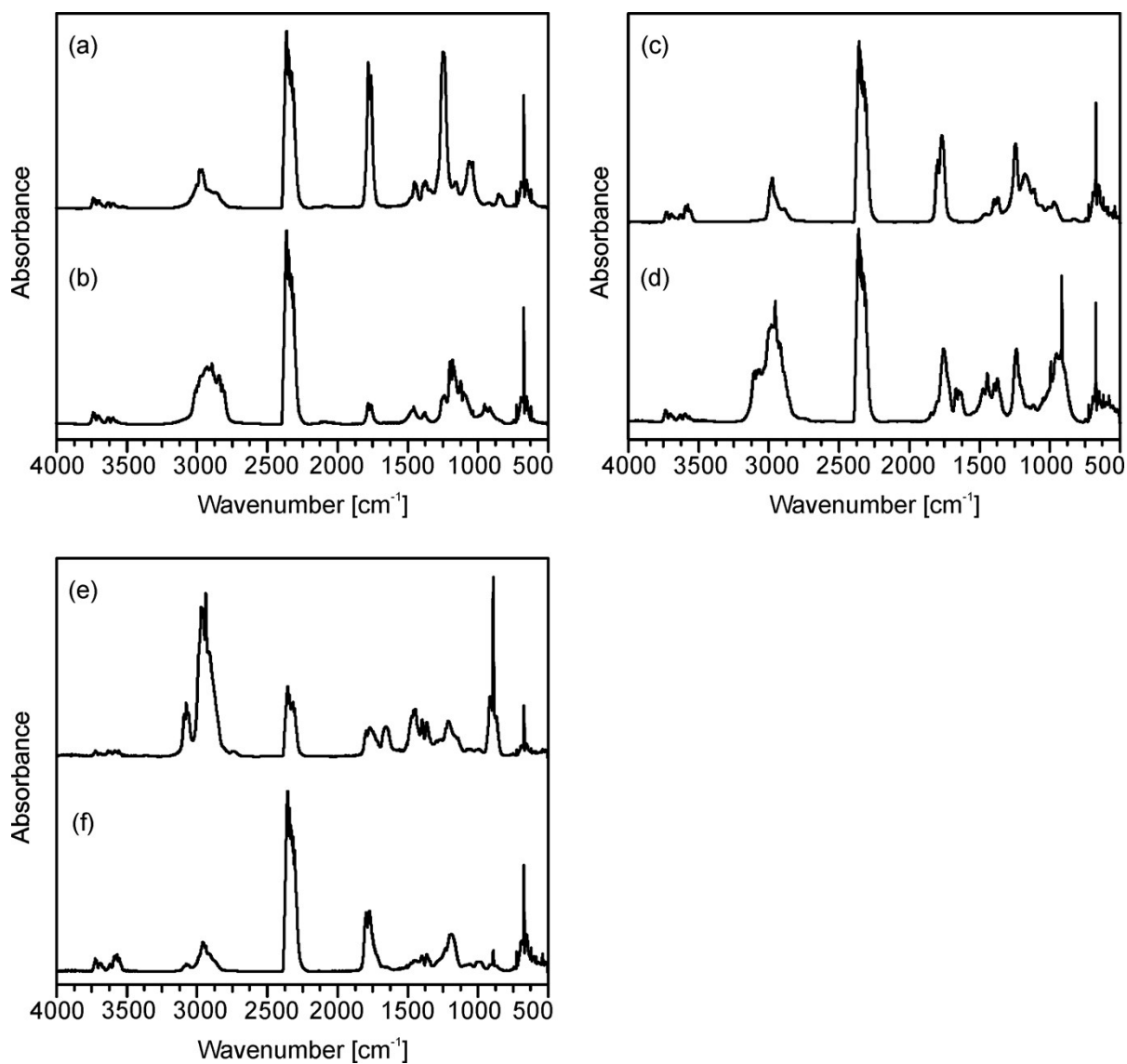
Microwave-assisted molecular solution based approach to potential high- κ -tantalum(V)oxide nanoparticles: Synthesis, dielectric properties and electron paramagnetic resonance spectroscopic studies of their defect chemistry.

Rudolf C. Hoffmann, Jörg J. Schneider*,

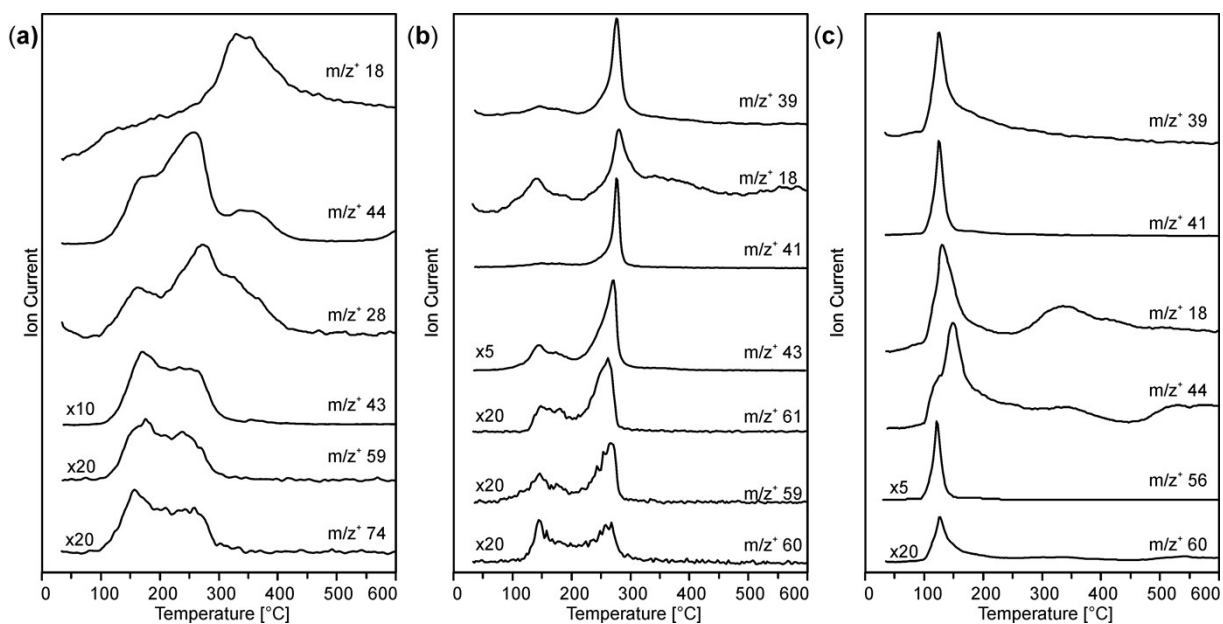
Mareiki Kaloumenos, Dieter Spiehl, Sergej Repp, Stefan Weber, Emre Erdem



Supplement Figure 1: TG mass loss curves as depicted in Figure 2 (continuous line) and corresponding Gram-Schmidt signals (dotted line) of (a) precursor (1), (b) precursor (2) and (c) precursor (3).



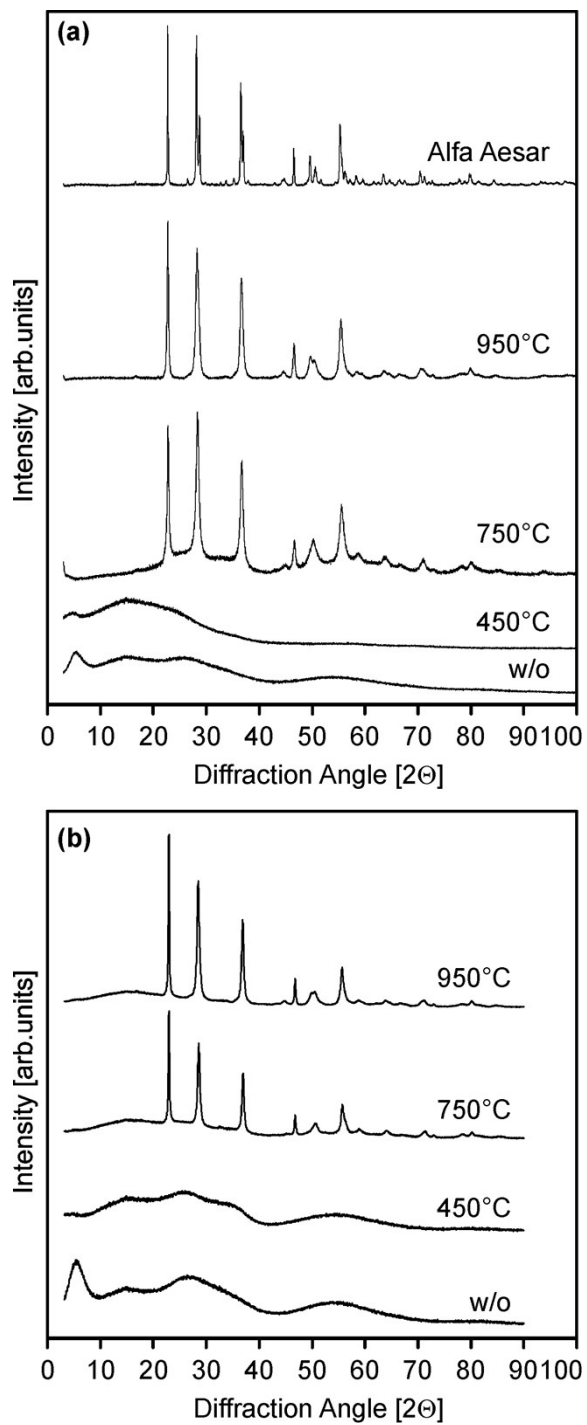
Supplement Figure 2: IR spectra of the gaseous decomposition products of (a)-(b) precursor (1), (c)-(d) precursor (2) as well as (e)-(f) precursor (3) corresponding to the first and second maximum in the Gram-Schmidt curve.



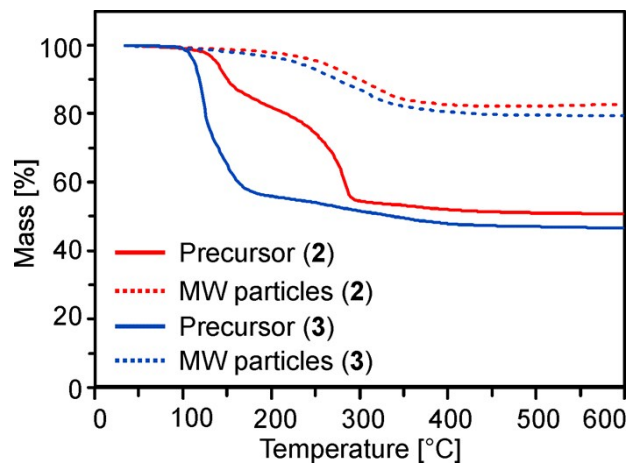
Supplement Figure 3: MS spectra of the gaseous decomposition products of (a) precursor (1), (b) precursor (2) and (c) precursor (3).

Precursor Concentration Weight %	Precursor (2) Z_{av}/nm (PI)	Precursor (3) Z_{av}/nm (PI)
2.5	3.5 (0.163)	5.3 (0.233)
5.0	4.3 (0.183)	6.5 (0.237)
7.5	5.6 (0.203)	20.4 (0.358)
10.0	6.8 (0.188)	36.8 (0.413)

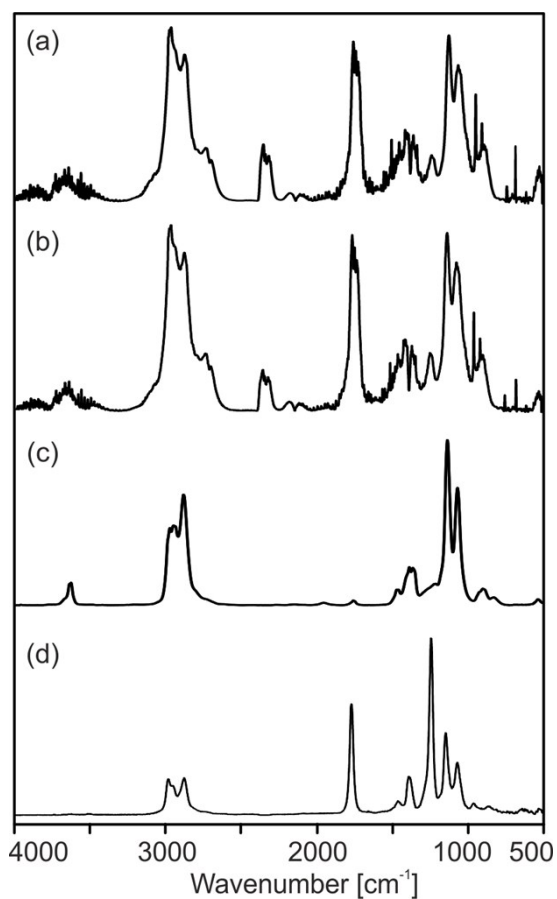
Supplement Table 1: Hydrodynamic diameters Z_{av} and polydispersity indices PI of particles obtained from the microwave reaction of various concentrations of the precursors (2) and (3).



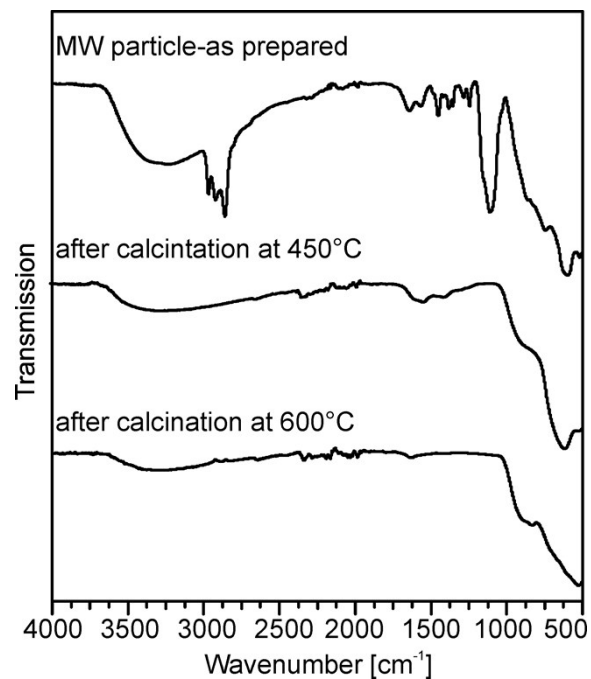
Supplement Figure 4: XRD patterns of powders obtained after microwave-reaction of (a) precursor (2) or (b) precursor (3) and additional calcination in air at various temperatures as well of a commercially available sample that was used as a reference in the EPR investigations (Supplement Figure 9).



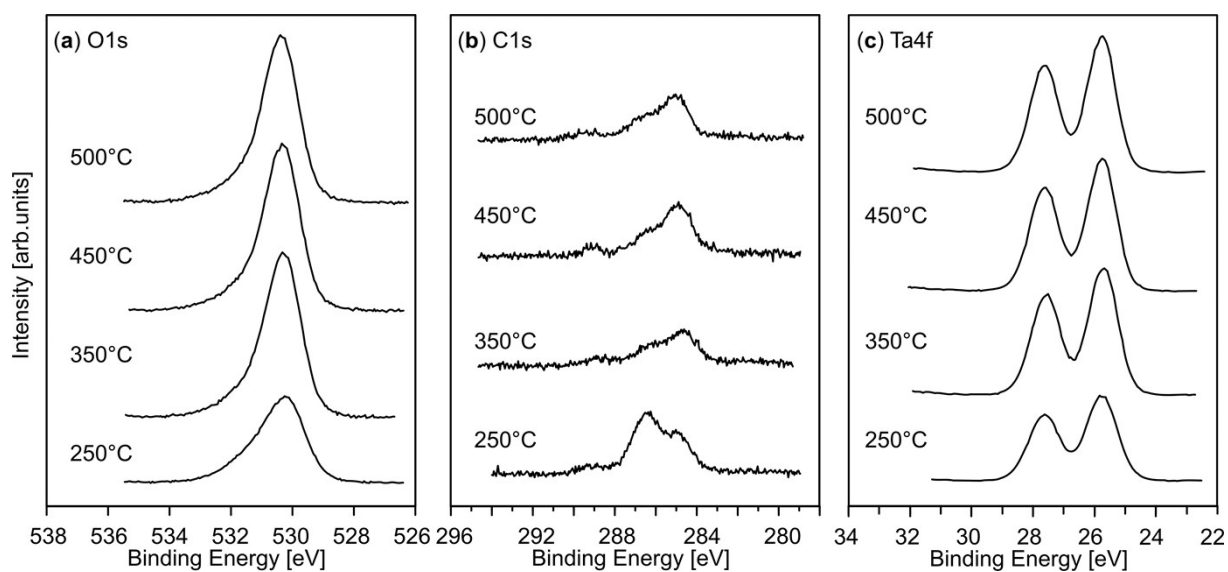
Supplement Figure 5: TG curves comparing the mass loss of precursors (2) and (3) with the corresponding powders obtained from microwave-reaction.



Supplement Figure 6: IR spectra of the gaseous decomposition products of powders obtained from (a) precursor (2) and (b) precursor (3) as well as reference spectra of (c) ethoxyethanol and (d) ethoxyethylacetate.



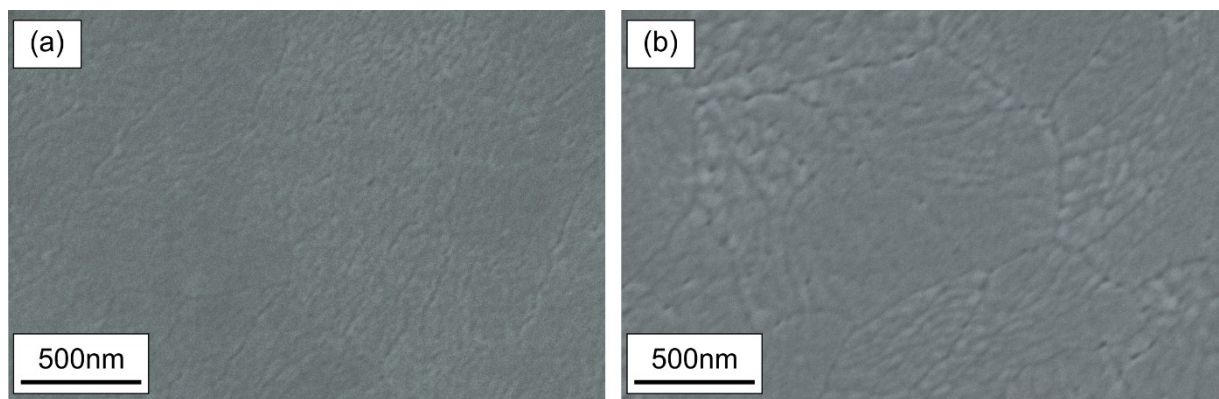
Supplement Figure 7: IR spectra of powders obtained from the microwave-reaction of precursor (**2**) and additional calcinations at various temperatures.



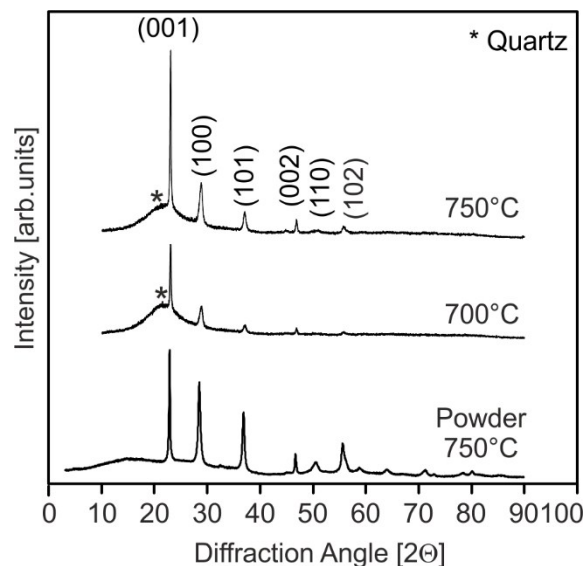
Supplement Figure 8: XPS spectra of films obtained from particles synthesized by the microwave-reaction of (**2**) after spincoating and additional calcination in air at various temperatures. (a) O 1s, (b) C 1s and (c) Ta 4f regime.

Sample	Area 4f _{7/2}	Area 4f _{5/2}	Ratio	Area 4f _{7/2}	Area 4f _{5/2}	Ratio	No.2/ No.1
250°C	13566	9588	1.41	283	330	0.85	0.021
350°C	16096	12519	1.28	365	246	1.48	0.023
450°C	16209	12679	1.27	414	320	1.29	0.026
500°C	16208	12597	1.28	389	352	1.10	0.024

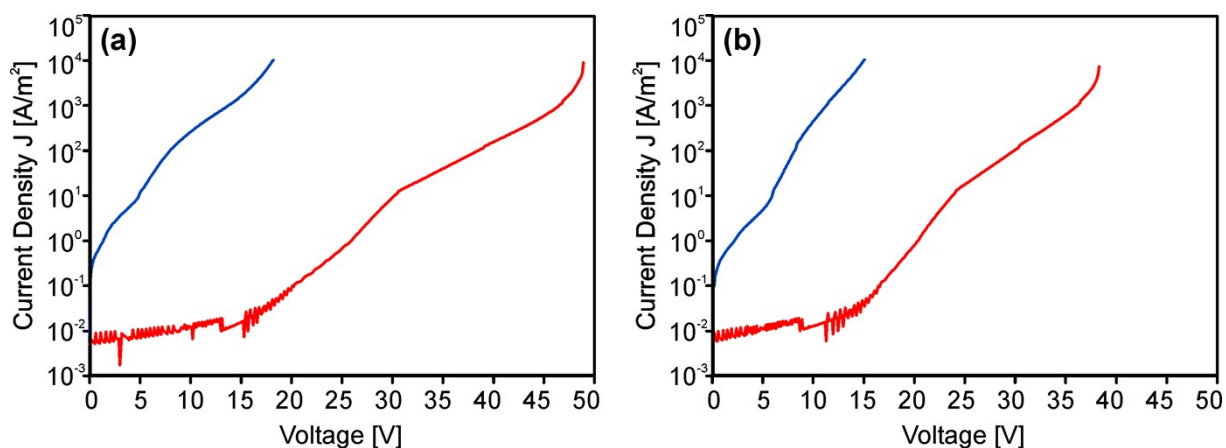
Supplement Table 2: Results for fitting procedure of XPS data. The theoretical value for the ratio of the areas underlying the 4f_{7/2} and 4f_{5/2} regimes for one component is 1.33. The first component is indicated in yellow, whereas a possible second component is highlighted in green. The ratio between these contributions is indicated in red.



Supplement Figure 9: SEM micrograph of thin films on quartz obtained by spin-coating of dispersions of particles from precursor (3) and annealing at 350 °C followed by sintering at (a) 700 and (b) 800 °C, respectively.



Supplement Figure 10: XRD patterns of thin films on quartz obtained by spin-coating of dispersions of particles from precursor **(3)** and annealing at 350 °C followed by sintering at 700 and 750 °C, respectively. The pattern of a powder from particles of derived from the same precursor after calcination at 750 °C (corresponds to Supplement Figure 4) is shown for comparison.



Supplement Figure 11: Leakage current density as function of voltage for tantalum oxide film after annealing at 350 °C in air (a) Particles synthesized from **(2)**, (b) Particles synthesized from **(3)**. Red curves refer to top electrodes with 250 μm width, whereas blue electrodes to 1000 μm. ITO bottom electrodes had 250 μm width in both cases. (The figures show typical curves.)

Supplementary information for EPR section:

Spin counting procedure:

To accurately count spins there are several important aspects that should be considered before and after the EPR experiment. Some issues are related to the spectrometer; others can be easily controlled by the EPR operator: (i) The sample weight needs to be carefully controlled. If it is not possible to have always the same sample amount in the EPR tube, then for normalization, each spectrum needs to be multiplied by a filling factor (deduced from the mass of the sample in the EPR tube). (ii) The sample should be accurately positioned in the center of the microwave cavity. (iii) If there is a background signal, then it is necessary to subtract it from the signal of the sample. (iv) One should always be careful not to saturate the EPR signal by applying too high microwave power. The microwave phase should be carefully adjusted during critical coupling (tuning) of the resonator. (v) One has to check whether there is a magnetic-field offset and calibrate the magnetic field if one is present. (vi) The Q value of the resonator has to be taken into account for all measurements, and spectra need to be normalized with respect to Q.

To calculate the defect concentration, one doubly integrates each first-derivative EPR signal. By comparing the integral of the standard sample (here, MnO powder) with the one from the sample of interest, one can obtain the corresponding number of spins, and from that the defect concentration. For a precise determination, one has to make a normalisation by taking into account the following expression including experimental parameters of both standard and the probe under investigation:

$$N_S^* \cdot \frac{RG^*}{RG} \cdot \frac{MF^*}{MF} \cdot \frac{MA^*}{MA} \cdot \frac{CT^*}{CT} \cdot \sqrt{\frac{P^*}{P}} \cdot \left(\frac{Scans^*}{Scans}\right)^2 \cdot \left(\frac{SW}{SW^*}\right)^2 \cdot \frac{S^*(S^*+1)}{S(S+1)} = \text{corrected value} \quad (1)$$

In this equation, N_S^* , RG , MF , MA , CT , P , $Scans$, SW , and S stand for the number of spins in standard sample, receiver-gain, modulation frequency [kHz], modulation amplitude [G], conversion time [ms], microwave-power [mW], field-sweep [G], number of scans, and spin quantum number, respectively. Note that, an asterisk indicates the measurement parameters for the standard sample. Once the normalised-corrected value of N_S^* is obtained, via simple cross multiplication of N_S^* and the area under the EPR signals, the defect

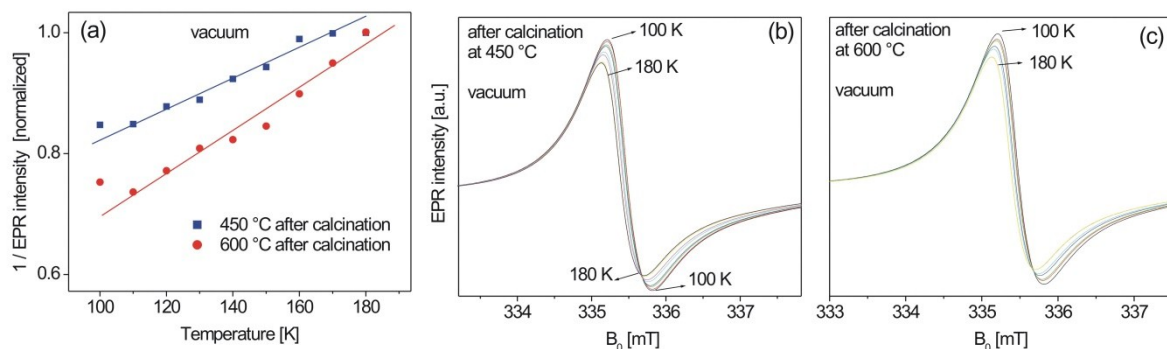
concentration, N_D , of the sample under investigation is obtained:

$$N_D = \frac{(Area)_D \cdot N_S^*}{(Area)^*} \quad (2)$$

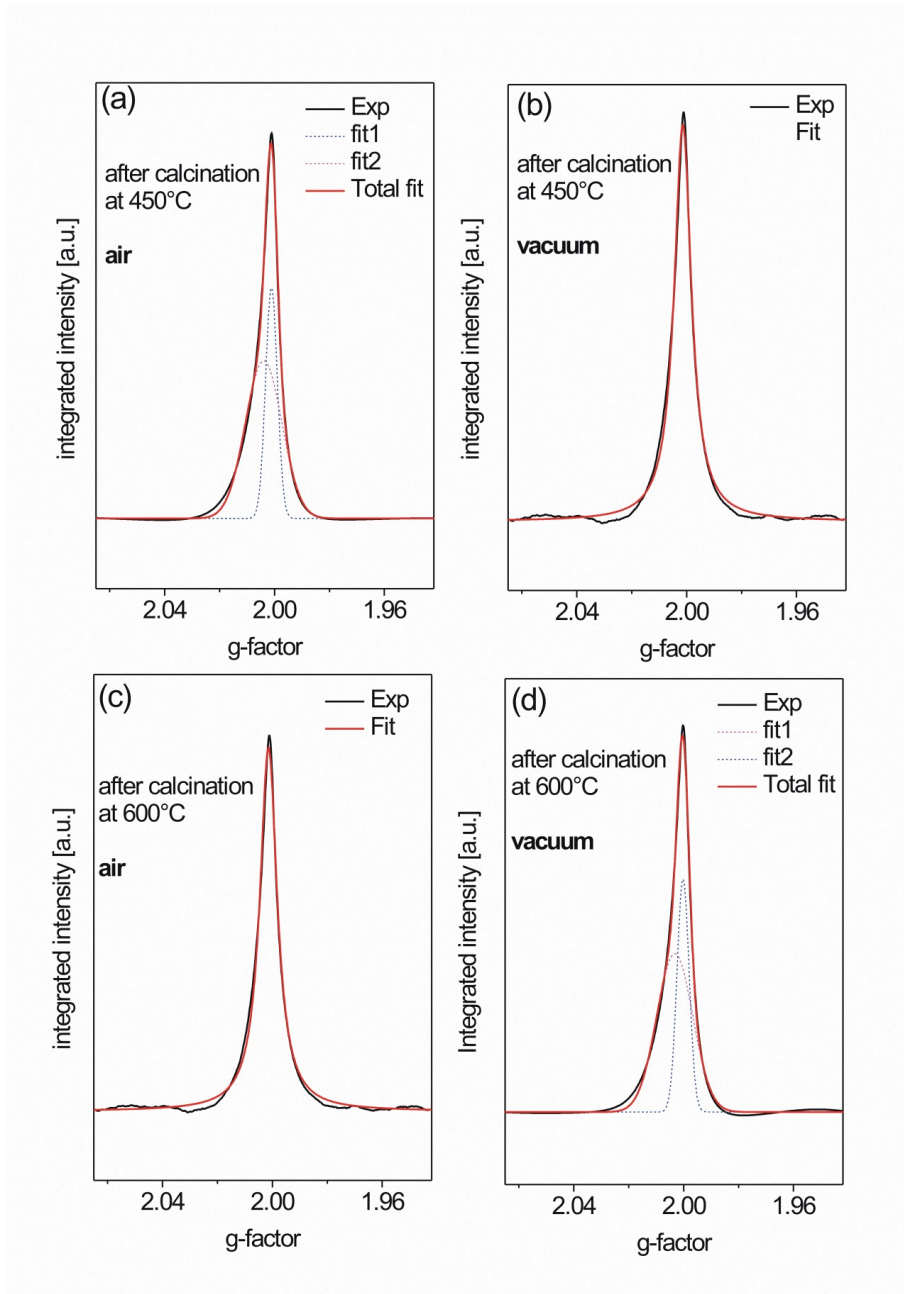
$(Area)_D$ and N_D are the area of the EPR signal of the related defect centre and the number of spins of the sample, respectively. In this work we used MnO powder as standard sample, which has 3.34×10^{19} spins/g.

Supplement Table 3: g-factors, corresponding EPR signal linewidths, and the spin concentration of defect centers in Ta₂O₅ deduced from the room-temperature cw-EPR spectra from spin counting.

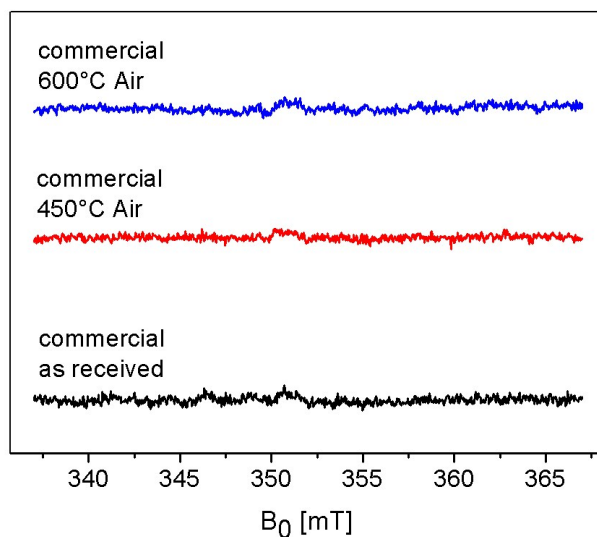
Sample	g-factor	Linewidth (G)	Defect concentration (spins/g)
as received (air)	2.0029(5)	11.4	9.85×10^{15}
450 °C (air)	2.0016(5)	5.7	1.63×10^{19}
600 °C (air)	2.0008(5)	5.7	1.40×10^{17}
450 °C (vacuum)	2.0016(5)	5.4	4.32×10^{19}
600 °C (vacuum)	2.0000(5)	5.2	3.97×10^{17}



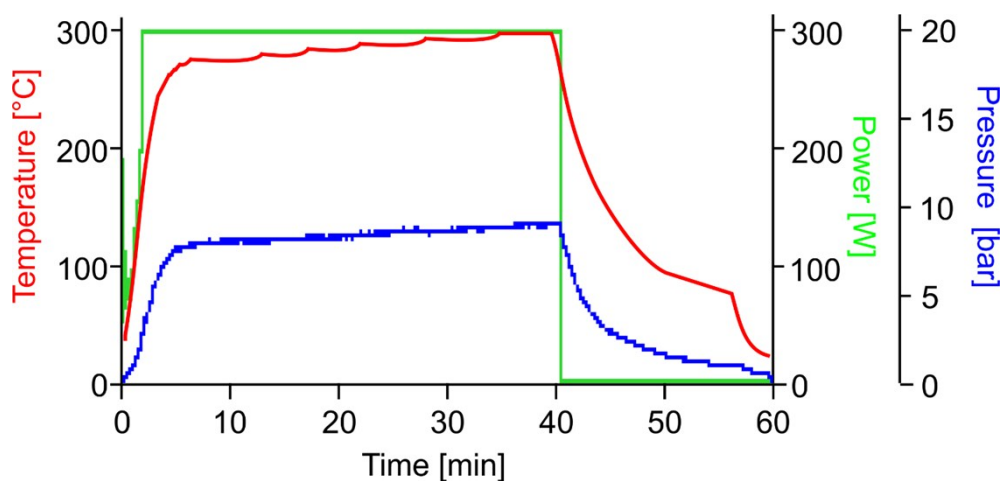
Supplement Figure 12: Temperature dependent EPR spectra. a) Reciprocal intensity vs temperature b) and c) measured spectra at temperatures between 100-180 K for 450 °C and 600 °C calcined samples under vacuum, respectively.



Supplement Figure 13: Integrated EPR spectra and their fits for all samples.



Supplement Figure 14: Cw-EPR spectra of commercial Ta₂O₅ powders: as-received and annealed 2 h at 450 and 600 °C.



Supplement Figure 15: Reaction conditions in the microwave depicting temperature, pressure and microwave power as a function of the reaction time. (The figure shows a typical sequence.)